



MPI-PTh 2-93  
TUM-T31-37/93  
January 1993

## QCD Corrections to Rare K- and B-Decays for Arbitrary Top Quark Mass\*

GERHARD BUCHALLA and ANDRZEJ J. BURAS

*Max-Planck-Institut für Physik  
- Werner-Heisenberg-Institut -  
P.O.Box 40 12 12, Munich (Fed. Rep. Germany)*

*Technische Universität München, Physik Department  
D-8046 Garching, Fed. Rep. Germany*

### ABSTRACT

We calculate strong interaction  $O(\alpha_s)$  corrections to rare K- and B-decays dominated by  $Z^0$ -penguins and box-diagrams with virtual top quark exchanges for an arbitrary top quark mass. We find that the uncertainty in the branching ratios, due to the dependence of  $m_t$  on the choice of the renormalization scale  $\mu$  is reduced from  $O(25\%)$  to  $O(3\%)$  by including the  $O(\alpha_s)$  corrections. For the choice  $\mu = m_t$  with  $100\text{GeV} \leq m_t \leq 200\text{GeV}$  the corrections to  $K_L \rightarrow \pi^0 \nu \bar{\nu}$  and  $B \rightarrow X_s \nu \bar{\nu}$  are less than 4% and at most 13% for  $B \rightarrow l \bar{l}$ . For the choice  $\mu = M_W$  they can be as large as 20% for both types of decays. We also point out that the published branching ratios for  $B \rightarrow l \bar{l}$  miss an overall factor of 2.

---

\*Supported by the German Bundesministerium für Forschung und Technologie under contract 06 TM 732 and by the CEC science project SC1-CT91-0729.

## 1. Introduction

In a recent paper [1] we have begun a systematic study of QCD corrections to rare one-loop induced K-meson and B-meson decays which are dominated by  $Z^0$ -penguin diagrams and box-diagrams. These decays being sensitive probes of the top quark couplings  $V_{td}$  and  $V_{ts}$  deserve particular attention, especially because the relevant branching ratios can be reliably calculated in the standard model. As we have stressed in [1] the pure electroweak contributions to these decays contain an unavoidable uncertainty due to the dependence of  $m_t$  on the choice of the renormalization scale  $\mu$ . Since the decays considered here are sensitive functions of  $m_t$ , this uncertainty is substantial and implies theoretical errors for branching ratios of  $O(25\%)$ . In order to reduce this uncertainty it is mandatory to calculate  $O(\alpha_s)$  corrections to diagrams involving internal top quark exchanges. Since the electroweak contributions appear at the one-loop level as shown in fig. 1, the inclusion of  $O(\alpha_s)$  QCD effects requires two loop calculations. These are rather tedious but in view of the possibility of extracting the couplings  $V_{ts}$  and  $V_{td}$  from the decays in question such an effort is justified in our opinion.

As a first step in this project we have calculated in [1] the  $O(\alpha_s)$  corrections to the one-loop induced  $\bar{s}dZ$ -vertex for an arbitrary top quark mass. This required the evaluation of 24 two-loop diagrams and of necessary QCD and electroweak counter-diagrams. We have found that the uncertainty in the strength of the effective vertex  $\bar{s}dZ$  due to the choice of scale  $\mu$  has been reduced from  $O(10\%)$  to  $O(1\%)$  by including the  $O(\alpha_s)$  corrections.

In order to complete the analysis of  $O(\alpha_s)$  corrections to relevant branching ratios also the QCD corrections to certain box diagrams have to be calculated. This will also remove the dependence on the W-boson gauge present in the effective vertex  $\bar{s}dZ$ . The purpose of the present paper is the calculation of the QCD corrections to box diagrams (b) and (c) of fig. 1 which contribute to decays with  $\nu\bar{\nu}$  and  $\mu\bar{\mu}$  in the final state respectively. Combining this calculation with the one of [1] we are able to construct QCD-corrected effective Hamiltonians for two classes of rare K- and B-decays which are dominated by internal top quark exchanges. In the case of

K-decays these two Hamiltonians are given explicitly as follows:

$$H_{eff}^{\nu\bar{\nu}} = \frac{G_F}{\sqrt{2}} \frac{\alpha}{2\pi \sin^2 \Theta_W} V_{ts}^* V_{td} X(x_t) (\bar{s}d)_{V-A} (\bar{\nu}\nu)_{V-A} \quad (1.1)$$

$$H_{eff}^{\mu\bar{\mu}} = -\frac{G_F}{\sqrt{2}} \frac{\alpha}{2\pi \sin^2 \Theta_W} V_{ts}^* V_{td} Y(x_t) (\bar{s}d)_{V-A} (\bar{\mu}\mu)_{V-A} \quad (1.2)$$

where  $x_t = m_t^2/M_W^2$ ,  $(\bar{s}d)_{V-A} \equiv \bar{s}\gamma_\mu(1-\gamma_5)d$ ,  $\alpha$  is the electromagnetic coupling constant and

$$X(x) = X_0(x) + \frac{\alpha_s}{4\pi} X_1(x) \quad (1.3)$$

$$Y(x) = Y_0(x) + \frac{\alpha_s}{4\pi} Y_1(x) \quad (1.4)$$

The scale of  $\alpha_s$  is  $O(M_W)$ . Next

$$X_0(x) = \frac{x}{8} \left[ -\frac{2+x}{1-x} + \frac{3x-6}{(1-x)^2} \ln x \right] \quad (1.5)$$

and

$$Y_0(x) = \frac{x}{8} \left[ \frac{4-x}{1-x} + \frac{3x}{(1-x)^2} \ln x \right] \quad (1.6)$$

represent pure electroweak one-loop contributions and  $X_1(x)$  and  $Y_1(x)$  resulting from  $O(g_2^4\alpha_s)$  two-loop diagrams are the functions calculated by us. They include the results of our previous paper [1]. We find

$$\begin{aligned} X_1(x) = & -\frac{23x+5x^2-4x^3}{3(1-x)^2} + \frac{x-11x^2+x^3+x^4}{(1-x)^3} \ln x \\ & + \frac{8x+4x^2+x^3-x^4}{2(1-x)^3} \ln^2 x - \frac{4x-x^3}{(1-x)^2} L_2(1-x) \\ & + 8x \frac{\partial X_0(x)}{\partial x} \ln x_\mu \end{aligned} \quad (1.7)$$

$$\begin{aligned} Y_1(x) = & \frac{4x+16x^2+4x^3}{3(1-x)^2} - \frac{4x-10x^2-x^3-x^4}{(1-x)^3} \ln x \\ & + \frac{2x-14x^2+x^3-x^4}{2(1-x)^3} \ln^2 x + \frac{2x+x^3}{(1-x)^2} L_2(1-x) \\ & + 8x \frac{\partial Y_0(x)}{\partial x} \ln x_\mu \end{aligned} \quad (1.8)$$

where  $x_\mu = \mu^2/M_W^2$

and

$$L_2(1-x) = \int_1^x dt \frac{\ln t}{1-t} \quad (1.9)$$

Here  $\mu$  is the scale at which the running top quark mass  $m_t(\mu)$  is defined. The  $\mu$ -dependences in the last terms in (1.7) and (1.8) cancel to the order considered the  $\mu$ -dependences in the leading terms  $X_0(x(\mu))$  and  $Y_0(x(\mu))$  respectively. It should be emphasized that the functions  $X_0, Y_0, X_1$  and  $Y_1$  are gauge independent.

The following sections give some details of the calculations which result in the formulae (1.7) and (1.8). In Section 2 we use the result of our previous paper [1] to construct the parts of the effective Hamiltonians coming from  $Z^0$ -penguin diagrams. In Section 3 we calculate  $O(\alpha_s)$  corrections to the box diagrams of fig. 1 and we construct the corresponding contributions to the effective Hamiltonians in question. In Section 4 we combine the results of the previous sections to obtain the complete Hamiltonians of eqs. (1.1) and (1.2). Subsequently we elaborate on the size of the  $O(\alpha_s)$  corrections with respect to the values of  $m_t$  and  $\mu$ . In particular we discuss the branching ratios for the decays  $K_L^0 \rightarrow \pi^0 \nu \bar{\nu}, B \rightarrow X_s \nu \bar{\nu}$  and  $B \rightarrow \bar{l} l$  which are dominated by internal top quark exchanges. We end our paper with a brief summary and with an outlook for corresponding calculations of the decays  $K^+ \rightarrow \pi^+ \nu \bar{\nu}$  and  $K_L \rightarrow \mu \bar{\mu}$  which receive additional contributions from internal charm quark exchanges. The latter require a somewhat different treatment due to  $m_c \ll M_W$  and will be analyzed in a separate publication.

## 2. Effective Hamiltonians from $Z^0$ -Penguins

In our previous paper [1] we have calculated the  $O(\alpha_s)$  corrections to the one-loop induced  $\bar{s}dZ$ -vertex for an arbitrary top quark mass. Including the  $Z^0$ -propagator and the tree-level coupling  $\bar{f}fZ^0$  with  $f$  denoting  $\mu$  or  $\nu$  we obtain after multiplication by  $i$  the parts of the effective Hamiltonians resulting from  $Z^0$ -penguin diagrams:

$$\Delta_Z H_{eff}^{\bar{f}f} = \frac{G_F}{\sqrt{2}} \frac{\alpha}{2\pi \sin^2 \Theta_W} V_{ts}^* V_{td} C(x_t) \cdot \left[ 2(T_3)_f (\bar{s}d)_{V-A} (\bar{f}f)_{V-A} - 4Q_f \sin^2 \Theta_W (\bar{s}d)_{V-A} (\bar{f}f)_V \right] \quad (2.1)$$

Here  $(T_3)_f$  is the third component of the weak isospin and  $Q_f$  is the electric charge of  $f$ . Only the first term in the parenthesis is of interest in this paper. The second

term contributes only to decays in which also photonic penguins are present. This is for instance the case of  $K_L \rightarrow \pi^0 e^+ e^-$ . The analysis of this process at this level would require also the calculation of  $O(\alpha_s)$  corrections to  $\gamma$ -penguins which is clearly beyond the scope of the present paper.

The function  $C(x)$  has been already analysed in detail in [1]. It is given as follows

$$C(x) = C_0(x) + \frac{\alpha_s}{4\pi} C_1(x) \quad (2.2)$$

where [2]

$$C_0(x) = \frac{x}{8} \left[ \frac{6-x}{1-x} + \frac{3x+2}{(1-x)^2} \ln x \right] \quad (2.3)$$

and [1]

$$\begin{aligned} C_1(x) = & \frac{29x + 7x^2 + 4x^3}{3(1-x)^2} - \frac{x - 35x^2 - 3x^3 - 3x^4}{3(1-x)^3} \ln x \\ & - \frac{20x^2 - x^3 + x^4}{2(1-x)^3} \ln^2 x + \frac{4x + x^3}{(1-x)^2} L_2(1-x) \\ & + 8x \frac{\partial C_0(x)}{\partial x} \ln x \mu \end{aligned} \quad (2.4)$$

As in (1.7) and (1.8)  $\mu$  is the scale at which the running top quark mass is defined and the last term in (2.4) cancels to the order considered the  $\mu$ -dependence present in the leading term  $C_0(x(\mu))$ . The function  $C(x)$  given here corresponds to 't Hooft-Feynman gauge for the  $W$ -propagator. In order to obtain gauge independent Hamiltonians also contributions from box diagrams have to be considered. This is what we will do next.

### 3. Effective Hamiltonians from Box-Diagrams

The effective Hamiltonians resulting from diagrams of figs. 1b, 1c and 2 are given as follows

$$\Delta_B H_{eff}^{\nu\bar{\nu}} = \frac{G_F}{\sqrt{2}} \frac{\alpha}{2\pi \sin^2 \Theta_W} V_{ts}^* V_{td} [-4B(x_t, 1/2)] (\bar{s}d)_{V-A} (\bar{\nu}\nu)_{V-A} \quad (3.1)$$

and

$$\Delta_B H_{eff}^{\mu\bar{\mu}} = \frac{G_F}{\sqrt{2}} \frac{\alpha}{2\pi \sin^2 \Theta_W} V_{ts}^* V_{td} B(x_t, -1/2) (\bar{s}d)_{V-A} (\bar{\mu}\mu)_{V-A} \quad (3.2)$$

where the second argument in the  $x_t$  dependent functions stands for  $(T_3)_f$ .

In the 't Hooft-Feynman gauge for W one has

$$B(x, \pm 1/2) = B_0(x) + \frac{\alpha_s}{4\pi} B_1(x, \pm 1/2) \quad (3.3)$$

with the one-loop function given by [2]

$$B_0(x) = \frac{1}{4} \left[ \frac{x}{1-x} + \frac{x}{(1-x)^2} \ln x \right] \quad (3.4)$$

The equality  $B(x, 1/2) = B(x, -1/2)$  at the one-loop level is a particular property of the 't Hooft-Feynman gauge. As we will see below this equality is violated by  $O(\alpha_s)$  corrections.

In order to find the  $O(\alpha_s)$  corrections in (3.3) we have to evaluate the diagrams of fig. 2, where generally charged virtual boson ( $W^\pm$ ) exchanges and fictitious Higgs particle ( $H^\pm$ ) exchanges have to be taken into account. In the case of  $\bar{s}d \rightarrow \mu\bar{\mu}$  however, the internal leptons are massless and in the approximation of neglecting the external masses only diagrams with  $W^\pm$  contribute. It turns out that in the case of internal top quark exchanges considered in the present paper it is an excellent approximation to set also  $m_e = m_\mu = m_\tau = 0$  in the process of evaluation of diagrams contributing to  $\bar{s}d \rightarrow \bar{\nu}\nu$ . Consequently also in this case only diagrams with internal  $W^\pm$  exchanges contribute which substantially simplifies the calculation. In the case of internal charm quark exchanges considered in our next paper  $m_\tau$  cannot be set to zero and the full set of diagrams with  $H^\pm$  and  $W^\pm$  has to be calculated. Consequently the function  $B(x, 1/2)$  given in the present paper is not valid for  $x = m_c^2/M_W^2$  and internal  $\tau$ -lepton exchange.

In [1] and in this paper we have used the program *TRACER* [3] written in *MATHEMATICA* [4] for the manipulation of the Dirac algebra. The many integrals present in our calculations have been evaluated in two ways: by hand and with the help of *MATHEMATICA* (G.B.) and independently (A.J.B.) by using the tables of Devoto and Duke [5] where *MACSYMA* [6] has been employed.

The diagrams (a) und (b) in fig. 2 are ultraviolet divergent but are infrared-finite. The diagram (c) is infrared-divergent. As in [1] we make use of the most convenient possibility, namely we choose external fermions as massless and on-shell. We then regularize all divergences dimensionally. As discussed in [1] such a treatment makes the factorization of short and long distance contributions essentially trivial. The  $O(\alpha_s)$  corrections to the matrix element of  $(\bar{s}d)_{V-A}$  vanish and the diagrams of fig. 1 and 2 give directly the Wilson coefficient functions.

The QCD counterterms necessary to make the diagrams of fig. 2 finite have been discussed at length in our previous paper and will not be given here. Electroweak counterterms are not present here because the one-loop diagrams are finite. The new feature of the diagrams of fig. 2 is the appearance of the Dirac structures like  $\gamma^\mu \gamma^\rho \gamma^\nu (1-\gamma_5) \otimes \gamma_\mu \gamma_\rho \gamma_\nu (1-\gamma_5)$  at the intermediate stages of the calculation. In  $D \neq 4$  dimensions such tensors can be rewritten as linear combinations of the operator  $(V-A) \otimes (V-A)$  and evanescent operators which vanish in  $D = 4$ . The latter could in principle give contributions when multiplied by  $1/\epsilon$  singularities. Yet this does not happen in the present calculation. In fact by adding the counterdiagrams it turns out that the coefficients multiplying the Dirac structures above can be made finite. The reduction to  $(V-A) \otimes (V-A)$  operators can then be made simply in  $D = 4$  dimensions.

There is a simple reason why the evanescent operators do not contribute here. The point is that the treatment of these operators at  $O(\alpha_s)$  depends generally on the renormalization scheme and this dependence can only be cancelled by two-loop anomalous dimensions. However, the current  $(\bar{s}d)_{V-A}$  has no anomalous dimensions and consequently also the contributions of evanescent operators must be absent.

Now the sum of the diagram 2a and of its counterdiagram gives a finite result. On the other hand the sum of the diagram 2b and of its counterdiagram is still divergent with the same property for the symmetric diagram. The left-over  $1/\epsilon$

divergence in 2b can be traced back to our treatment of external lines (massless, on-shell) for which the  $O(\alpha_s)$  term in the field renormalization constant is absent in dimensional regularization as discussed in [1]. It is then not surprising that the left-over  $1/\epsilon$  divergences in 2b and in its symmetric counterpart are precisely cancelled by the infrared  $1/\epsilon$  singularity present in the diagram 2c. It turns out that the sum of diagrams of fig. 2 contains  $x$ -independent terms. These terms will be dropped in what follows because they are cancelled by the GIM mechanism anyway. Summing all contributions we obtain the result for the  $O(\alpha_s)$  corrections in (3.3)

$$B_1(x, 1/2) = \frac{13x + 3x^2}{3(1-x)^2} - \frac{x - 17x^2}{3(1-x)^3} \ln x - \frac{x + 3x^2}{(1-x)^3} \ln^2 x + \frac{2x}{(1-x)^2} L_2(1-x) + 8x \frac{\partial B_0(x)}{\partial x} \ln x_\mu \quad (3.5)$$

and

$$B_1(x, -1/2) = \frac{25x - 9x^2}{3(1-x)^2} + \frac{11x + 5x^2}{3(1-x)^3} \ln x - \frac{x + 3x^2}{(1-x)^3} \ln^2 x + \frac{2x}{(1-x)^2} L_2(1-x) + 8x \frac{\partial B_0(x)}{\partial x} \ln x_\mu \quad (3.6)$$

As in the case of  $C(x)$ , the last terms in (3.5) and (3.6) cancel to the order considered the  $\mu$ -dependence present in the leading term  $B_0(x(\mu))$ .

We note that the difference between  $B_1(x, 1/2)$  and  $B_1(x, -1/2)$  is very simple:

$$B_1(x, -1/2) - B_1(x, 1/2) = 16B_0(x) \quad (3.7)$$

Next we would like to consider the limiting cases  $x \ll 1$  and  $x \gg 1$ . In the case  $x \ll 1$ , which will be relevant for the charm contribution, one can perform a leading-log renormalization group analysis [7, 8, 9] and obtain a QCD correction factor  $\eta_B$  for the leading term in the  $B_0$ -function:

$$B_0 \rightarrow \frac{1}{4} x \ln x \cdot \eta_B \quad (3.8)$$

$\eta_B$  contains the sum of all leading logarithmic corrections. If we retain only the  $O(\alpha_s)$ -term we can write ( $K = \alpha_s(M_W)/\alpha_s(m)$ )

$$\eta_B = \frac{6\pi}{\alpha_s(m) \ln \frac{M_W}{m}} (1 - K^{1/23}) \doteq 1 + \frac{\alpha_s}{4\pi} 4 \ln x \quad (3.9)$$

Then (3.8) coincides, as it should, with the  $x \ll 1$  limit ( $\mu = m$ )

$$B_0 + \frac{\alpha_s}{4\pi} B_1(x, \pm 1/2) \rightarrow \frac{1}{4} x \ln x + \frac{\alpha_s}{4\pi} x \ln^2 x \quad (3.10)$$

which provides a certain check of our two-loop calculations.

In the limit  $x \gg 1$  the functions  $B$  tend to a constant, in the contrary to  $C$  which grows essentially proportional to  $x$ . Therefore the leading terms as  $x \rightarrow \infty$  are the same for the functions  $X$  and  $Y$  and equal to the leading terms of  $C$  which may be found in [1].

#### 4. Total Hamiltonians and Applications

Combining the results of Sections 2 and 3 we find the effective Hamiltonians (1.1) and (1.2) with

$$X(x_t) = C(x_t) - 4B(x_t, 1/2) \quad (4.1)$$

$$Y(x_t) = C(x_t) - B(x_t, -1/2) \quad (4.2)$$

from which formulae (1.5) – (1.8) follow.

Let us first investigate the size of the  $O(\alpha_s)$  corrections in (1.3) and (1.4). To this end we take  $\Lambda_{QCD} = 200 MeV$ . Since the scale of  $\alpha_s$  is  $O(M_W)$ , the corrections are rather insensitive to the value of  $\Lambda_{QCD}$  and very similar results are obtained for  $100 MeV \leq \Lambda_{QCD} \leq 300 MeV$ . For the running quark mass we use the leading log expression

$$m^2(\mu) = m^2(m) \left[ \frac{\alpha_s(\mu)}{\alpha_s(m)} \right]^{\frac{24}{23}} \quad (4.3)$$

In fig. 3 we plot the ratio  $(\alpha/4\pi)X_1/X_0$  for two choices of  $\mu$ ,  $\mu = m_t$  and  $\mu = M_W$ , as a function of  $m_t$ . As anticipated in [1] and in Section 3 for  $\mu = m_t$  the correction is small in the full range of  $m_t$  considered and very weakly dependent on  $m_t$ . It varies from  $-1.9\%$  for  $m_t = 90 GeV$  to  $-1.6\%$  for  $m_t = 300 GeV$ . Thus for high values of  $m_t$  the lowest order function  $X_0(x)$  represents well the QCD-corrected result when interpreted as  $X_0(x(\mu = m_t))$ .

On the other hand if the choice  $\mu = M_W$  is made, the correction is substantial and varies from  $-3\%$  for  $m_t = 90 GeV$  to  $-17\%$  for  $m_t = 300 GeV$ . For instance for

$m_t = 150\text{GeV}$  it amounts to  $-8\%$ . This sizeable negative correction for  $m_t \gg M_W$  compensates the “artificial” growth of  $X_0(x)$  when the scale  $\mu$  is unnaturally lowered to  $\mu = M_W \ll m_t$ .

Consequently when QCD corrections have been taken into account the final result for  $X(x)$  is essentially the same irrespective of whether  $\mu = m_t$  or  $\mu = M_W$  has been chosen. This situation should be contrasted with the zero order result  $X(x) = X_0(x)$  which sensitively depends on the choice of  $\mu$ . We will demonstrate this explicitly on the examples of branching ratios.

Similar features are observed in the case of the function  $Y(x)$  as illustrated in fig. 4 and in the analysis below, although all effects are larger than in the case of  $X(x)$ . This is partly related to the stronger dependence of  $Y(x)$  on  $x$ .

The effects just discussed are more pronounced when specific branching ratios are considered. As the first example we calculate the branching ratio for the CP-violating decay  $K_L \rightarrow \pi^0 \nu \bar{\nu}$  [9, 10, 11]. Summing over three neutrino flavours one has

$$B(K_L \rightarrow \pi^0 \nu \bar{\nu}) = 1.94 \cdot 10^{-10} \eta^2 A^4 \left[ X_0^2(x_t) + \frac{\alpha_s}{2\pi} X_0(x_t) X_1(x_t) \right] \quad (4.4)$$

where we have dropped consistently  $O(\alpha_s^2)$  terms.

$A$  and  $\eta$  are the Wolfenstein parameters. Taking typical values  $A = 0.85$  and  $\eta = 0.40$  and setting  $m_t(m_t) = 150\text{GeV}$  we plot in fig. 5  $B(K_L \rightarrow \pi^0 \nu \bar{\nu})$  with and without QCD corrections as a function of  $\mu$ . We observe that the inclusion of  $O(\alpha_s)$  corrections reduces the ambiguity due to the choice of  $\mu$  from  $O(20\%)$  to roughly 2–3% thus considerably increasing the predictive power of the theory. Varying  $\mu$  in the range from  $90\text{GeV}$  to  $290\text{GeV}$  one finds that for the above choice of  $m_t$ ,  $A$  and  $\eta$  the uncertainty in  $B(K_L \rightarrow \pi^0 \nu \bar{\nu})$ :

$$2.65 \cdot 10^{-11} \leq B(K_L \rightarrow \pi^0 \nu \bar{\nu}) \leq 3.25 \cdot 10^{-11} \quad (4.5)$$

present in the leading order is reduced to

$$2.80 \cdot 10^{-11} \leq B(K_L \rightarrow \pi^0 \nu \bar{\nu}) \leq 2.88 \cdot 10^{-11} \quad (4.6)$$

when the QCD corrections are taken into account.

At present the value of  $A$  extracted from  $b \rightarrow c$  transitions is given roughly by  $A \simeq 0.85 \pm 0.12$  and the error on  $\eta$  obtained from the parameter  $\epsilon_K$  is considerably

larger. Consequently the usefulness of the results obtained in the present paper is damped by the uncertainties in  $\eta$ ,  $A$  and in the value of  $m_t(m_t)$ . Once the top quark has been discovered,  $m_t(m_t)$  measured and the error on  $A$  substantially reduced, a measurement of  $B(K_L \rightarrow \pi^0 \nu \bar{\nu})$  if at all possible, should give in conjunction with our calculations a reliable estimate of the parameter  $\eta$ . We are aware of the fact that it may take a decade or more to achieve this goal.

A similar discussion can be made for the decay  $B \rightarrow X_s \Sigma \nu \bar{\nu}$  which is also governed by the function  $X(x_t)$ . This decay offers probably the cleanest way to measure the coupling  $V_{ts}$ . Its branching ratio is given as [10]

$$\frac{B(B \rightarrow X_s \Sigma \nu \bar{\nu})}{B(B \rightarrow X_c e \bar{\nu}_e)} = 3 \frac{\alpha^2}{4\pi^2 \sin^4 \Theta_W} \frac{|V_{ts}|^2}{|V_{cb}|^2} \frac{X_0^2(x_t) + \frac{\alpha_s}{2\pi} X_0(x_t) X_1(x_t)}{f(m_c/m_b) \eta_0} \quad (4.7)$$

where  $f(m_c/m_b) \simeq 0.44$  is a phase-space factor in  $B \rightarrow X_c e \bar{\nu}_e$  and  $\eta_0 \simeq 0.87$  is the corresponding QCD correction for  $\Lambda_{QCD} = 200 \text{ MeV}$  [12].

Taking  $|V_{ts}| = |V_{cb}|$ ,  $\alpha = 1/128$ ,  $\sin^2 \Theta_W = 0.23$ ,  $B(B \rightarrow X_c e \bar{\nu}_e) = 11\%$  and  $m_t(m_t) = 150 \text{ GeV}$  and varying  $\mu$  in the range  $90 \text{ GeV} \leq \mu \leq 290 \text{ GeV}$  we find that the uncertainty

$$4.15 \cdot 10^{-5} \leq B(B \rightarrow X_s \Sigma \nu \bar{\nu}) \leq 5.08 \cdot 10^{-5} \quad (4.8)$$

present in the leading order is reduced to

$$4.37 \cdot 10^{-5} \leq B(B \rightarrow X_s \Sigma \nu \bar{\nu}) \leq 4.49 \cdot 10^{-5} \quad (4.9)$$

after the inclusion of QCD corrections.

As an example of a decay governed by the function  $Y(x_t)$  we consider the decay  $B_s^0 \rightarrow l \bar{l}$  for which we find

$$B(B_s \rightarrow l \bar{l}) = \tau(B_s) \frac{G_F^2}{\pi} \left( \frac{\alpha}{4\pi \sin^2 \Theta_W} \right)^2 F_B^2 m_l^2 m_B \sqrt{1 - 4 \frac{m_l^2}{m_B^2}} |V_{ts}^* V_{tb}|^2 \cdot \left[ Y_0^2(x_t) + \frac{\alpha_s}{2\pi} Y_0(x_t) Y_1(x_t) \right] \quad (4.10)$$

where  $B_s$  denotes the flavor eigenstate ( $\bar{s}b$ ). The  $B$ -meson decay constant  $F_B$  is defined through

$$\langle 0 | (\bar{s}b)_{V-A, \mu} | B_s(p) \rangle = i F_B p_\mu \quad (4.11)$$

which corresponds to  $F_\pi = 132MeV$ .  $\tau(B_s)$  is the  $B_s$ -meson lifetime. Formula (4.10) in addition to the inclusion of  $O(\alpha_s)$  terms corrects for an overall factor of 2 missing in the existing literature [10,13,14]. A similar expression for the decay of the  $K_L$ -analogue of the  $B^0$ -meson in the limit  $x_t \ll 1$  has however been correctly given in [15].

Considering the decay  $B_s \rightarrow \mu\bar{\mu}$  we have numerically

$$B(B_s \rightarrow \mu\bar{\mu}) = 2.4 \cdot 10^{-9} \frac{\tau(B_s)}{1.28ps} \left[ \frac{F_B}{200MeV} \right]^2 \left[ \frac{|V_{ts}|}{0.041} \right]^2 \left[ Y_0^2(x_t) + \frac{\alpha_s}{2\pi} Y_0(x_t)Y_1(x_t) \right] \quad (4.12)$$

Taking the central values for  $\tau(B_s)$ ,  $F_B$  and  $|V_{ts}|$  we plot  $B(B_s \rightarrow \mu\bar{\mu})$  in fig. 6 for the cases considered in fig. 5. All the features seen in fig. 5 are also clearly visible here although the effects are stronger. The ambiguity of  $O(30\%)$  present in the leading order is decreased to roughly 2% after the inclusion of  $O(\alpha_s)$  corrections.

In analogy to (4.5) and (4.6) we have, without and including the QCD correction

$$1.44 \cdot 10^{-9} \leq B(B \rightarrow \mu\bar{\mu}) \leq 1.91 \cdot 10^{-9} \quad (4.13)$$

and

$$1.76 \cdot 10^{-9} \leq B(B \rightarrow \mu\bar{\mu}) \leq 1.79 \cdot 10^{-9} \quad (4.14)$$

respectively.

Finally in Table 1 we give the values for the ratios

$$\eta_X = \frac{X(x_t)}{X_0(x_t)} \quad \eta_Y = \frac{Y(x_t)}{Y_0(x_t)} \quad (4.15)$$

as functions of  $m_t$  for the choices  $\mu = m_t$  and  $\mu = M_W$ . Again  $\Lambda_{QCD} = 200MeV$  has been used but almost identical results are obtained in the full range  $100MeV \leq \Lambda_{QCD} \leq 300MeV$ . This table is a different representation of the features found in figs. 3 and 4 and should be useful in phenomenological applications.

$m_t/GeV$	$\eta_X = X/X_0$		$\eta_Y = Y/Y_0$	
	$\mu = m_t$	$\mu = M_W$	$\mu = m_t$	$\mu = M_W$
<b>90</b>	0.981	0.970	1.072	1.057
<b>110</b>	0.983	0.952	1.054	1.014
<b>130</b>	0.984	0.937	1.042	0.979
<b>150</b>	0.984	0.922	1.032	0.951
<b>170</b>	0.985	0.908	1.025	0.926
<b>190</b>	0.985	0.895	1.019	0.904
<b>210</b>	0.985	0.882	1.015	0.885
<b>230</b>	0.985	0.869	1.011	0.867
<b>250</b>	0.985	0.856	1.008	0.850
<b>270</b>	0.984	0.844	1.005	0.835
<b>290</b>	0.984	0.832	1.002	0.820

Table 1

## 5. Summary and Outlook

We have presented the first calculation of the  $O(\alpha_s)$  corrections to rare  $K$ - and  $B$ -decays dominated by top-quark exchanges in  $Z^0$ -penguin and box diagrams. Our calculations are valid to all orders in the internal quark mass ratio  $x_t = m_t^2/M_W^2$  and go beyond the previous studies of QCD corrections to these decays [7, 8, 9]. An important ingredient in our work was the calculation of the  $O(\alpha_s)$  correction to the effective low energy FCNC vertex  $\bar{s}dZ$  presented in [1]. The main results of [1] and of this paper can be summarized as follows:

- The QCD-corrected Hamiltonians, given in (1.1) and (1.2).
- The QCD-corrected effective vertex  $\bar{s}dZ$  obtained in the 't Hooft-Feynman gauge, given in (1.1) of [1].
- The  $O(\alpha_s)$  calculations allow to resolve to a large extent the quite sizable ambiguity in the lowest order expressions due to the dependence of  $m_t$  on the (arbitrary) renormalization scale  $\mu$ . The related uncertainty in the branching

ratios is reduced from  $O(25\%)$  to less than 3% when QCD corrections are taken into account.

- The  $O(\alpha_s)$  corrections to leading order results are made small for large  $m_t$  when the renormalization scale is chosen as  $\mu = m_t$ , i.e. the running top quark mass is defined as  $m_t = m_t(m_t)$ . For the expected range of values of the top quark mass  $130\text{GeV} \leq m_t(m_t) \leq 190\text{GeV}$ , the QCD factors  $\eta_X$  and  $\eta_Y$  defined in (4.15) are essentially independent of  $m_t$  and  $\Lambda_{QCD}$  and given by

$$\eta_X \simeq 0.985 \quad 1.019 \leq \eta_Y \leq 1.042 \quad (5.1)$$

If  $\mu = M_W$  is chosen one finds  $0.895 \leq \eta_X \leq 0.937$  and  $0.904 \leq \eta_Y \leq 0.979$  for the same range of top quark masses, as can be seen in Table 1. Similar features have been found in [16] where next-to-leading order QCD corrections to  $B^0 - \bar{B}^0$  mixing have been calculated. Also in this case the choice  $\mu = m_t$  led to a substantial reduction of the next-to-leading corrections and the corresponding QCD factor  $\eta_2$  was essentially independent of  $m_t$  for this choice of  $\mu$ :  $\eta_2 \simeq 0.55$ .

- The QCD corrected functions  $X(x)$  and  $Y(x)$  of (1.3) and (1.4) are central in the penguin-box expansion formulated by us some time ago [9]. The present work is a non-trivial step towards the generalization of this expansion beyond the leading order.

We have illustrated various aspects of our calculations by considering the branching ratios  $B(K_L \rightarrow \pi^0 \nu \bar{\nu})$ ,  $B(B \rightarrow X_s \Sigma \nu \bar{\nu})$  and  $B(B \rightarrow l \bar{l})$ . We are aware of the fact that while these decays give us an excellent laboratory for the study of QCD effects in rare decays, it will take at least a decade before these particular decays can be experimentally detected and our results tested. In this respect the calculation of QCD corrections to the decay  $K^+ \rightarrow \pi^+ \nu \bar{\nu}$  is of more interest, because there is a chance that this decay will be observed in the near future. The QCD corrected top-quark contributions to this decay can already be obtained by using the Hamiltonian (1.1). It is however known that this decay receives important contributions from internal charm exchanges. In view of  $m_c \ll M_W$ , large logarithms  $\ln M_W/m_c$  present in these contributions must be summed up by means of renormalization group techniques. The leading log analyses of charm contributions are

known [7, 8, 9]. However, in order to be consistent with the  $O(\alpha_s)$ -top quark contributions calculated here, a next-to-leading log calculation in the charm sector has to be performed. Such a calculation should reduce considerably the uncertainty in  $B(K^+ \rightarrow \pi^+ \nu \bar{\nu})$  due to the choice of the value of the charm quark mass [17, 18] and due to non-leading mass terms. Similar comments apply to the short distance part of  $B(K_L \rightarrow \mu \bar{\mu})$ . The next-to-leading log analysis of these decays is in progress.

#### ACKNOWLEDGEMENTS

We thank A. Ali, C. Greub and T. Mannel for the prompt confirmation of the factor of 2 in (4.10).

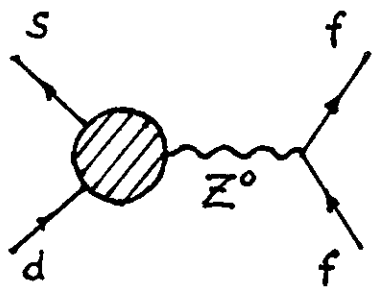
## REFERENCES

- [1] G. Buchalla and A. J. Buras, QCD Corrections to the  $\bar{s}dZ$ -Vertex for Arbitrary Top Quark Mass, MPI-PTh 111-92, TUM-T31-36/92.
- [2] T. Inami and C.S. Lim, *Progr. Theor. Phys.* **65** (1981) 297; *ibid* **65** (1981) 1772.
- [3] M. Jamin and M. E. Lautenbacher, Technical University Munich preprint, TUM-T31-20/91 (1991), to appear in *Comp. Phys. Comm.*.
- [4] S. Wolfram, *MATHEMATICA* – A System for Doing Mathematics by Computer, Addison-Wesley Publishing Company Inc., 1991.
- [5] A. Devoto and D. W. Duke, Florida State University preprint, FSU-HEP-831003.
- [6] *MACSYMA* Reference Manual, The Mathlab Group, Laboratory for Computer Science, MIT (1983).
- [7] J. Ellis and J.S. Hagelin, *Nucl. Phys.* **B 217** (1983) 189; V.A. Novikov, M.A. Shifman, A.I. Vainshtein and V.I. Zakharov, *Phys. Rev.* **D 16** (1977) 223.
- [8] C.O. Dib, I. Dunietz and F.J. Gilman, *Mod. Phys. Lett.* **A6** (1991) 3573.
- [9] G. Buchalla, A.J. Buras and M.K. Harlander, *Nucl. Phys.* **B 349** (1991) 1; G. Buchalla, Diploma-Thesis (1990), unpublished.
- [10] A.J. Buras and M.K. Harlander, A Top Quark Story, in Heavy Flavours, eds. A.J. Buras and M. Lindner, World Scientific (1992), page 58.
- [11] L. S. Littenberg, *Phys. Rev.* **D 39** (1989) 3322.
- [12] N. Cabibbo and L. Maiani, *Phys. Lett.* **B 79** (1978) 109.
- [13] B. A. Campbell and P. J. O' Donnell, *Phys. Rev.* **D 25** (1982) 1989.
- [14] A. Ali, Rare Decays of B-Mesons, DESY 91-080 (1991).

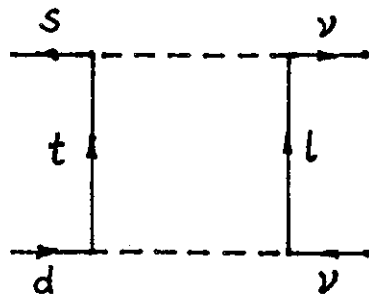
- [15] T. G. Rizzo, *Phys. Rev. D* **21** (1980) 2692.
- [16] A.J. Buras, M. Jamin and P.H. Weisz, *Nucl. Phys. B* **347** (1990) 491.
- [17] C. O. Dib, UCLA/91/TEP/45.
- [18] G. R. Harris and J. L. Rosner, *Phys. Rev. D* **45** (1992) 946.

## Figure Captions

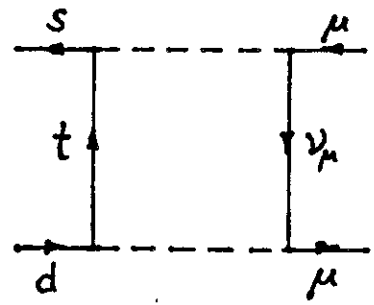
- Fig. 1** The leading one-loop diagrams contributing to the transitions  $\bar{s}d \rightarrow \bar{\nu}\nu$  and  $\bar{s}d \rightarrow \bar{\mu}\mu$ . The dashed lines represent  $W^\pm$ . The corresponding fictitious Higgs exchanges are absent in the case of vanishing lepton masses.
- Fig. 2** The  $O(\alpha_s)$  gluonic corrections to the box diagrams of fig. 1 (b) and (c).
- Fig. 3** The relative correction to the leading result  $X_0$  as a function of  $m_t(\mu)$  for the two cases  $\mu = M_W$  (dashed line) and  $\mu = m_t$  (solid line).
- Fig. 4** The same as in fig. 3 for  $Y$ .
- Fig. 5** The  $\mu$ -dependence of the branching ratio  $B(K_L \rightarrow \pi^0\nu\bar{\nu})$  with (solid) and without (dashed) QCD corrections for  $m_t(m_t) = 150\text{GeV}$ ,  $A = 0.85$  and  $\eta = 0.40$ .
- Fig. 6** The same as in fig. 5 for  $B(B_s \rightarrow \mu\bar{\mu})$  with  $\tau(B_s) = 1.28\text{ps}$ ,  $F_B = 200\text{MeV}$  and  $|V_{ts}| = 0.041$ .



(a)

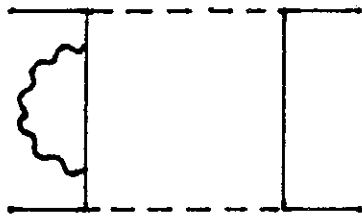


(b)

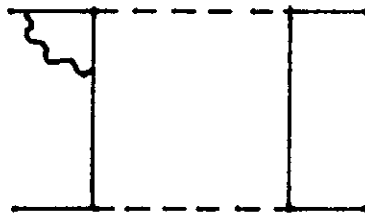


(c)

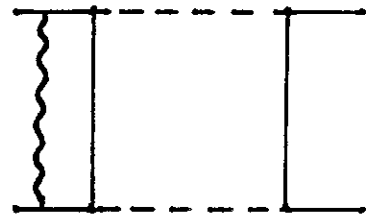
Fig. 1



(a)



(b)



(c)

Fig. 2

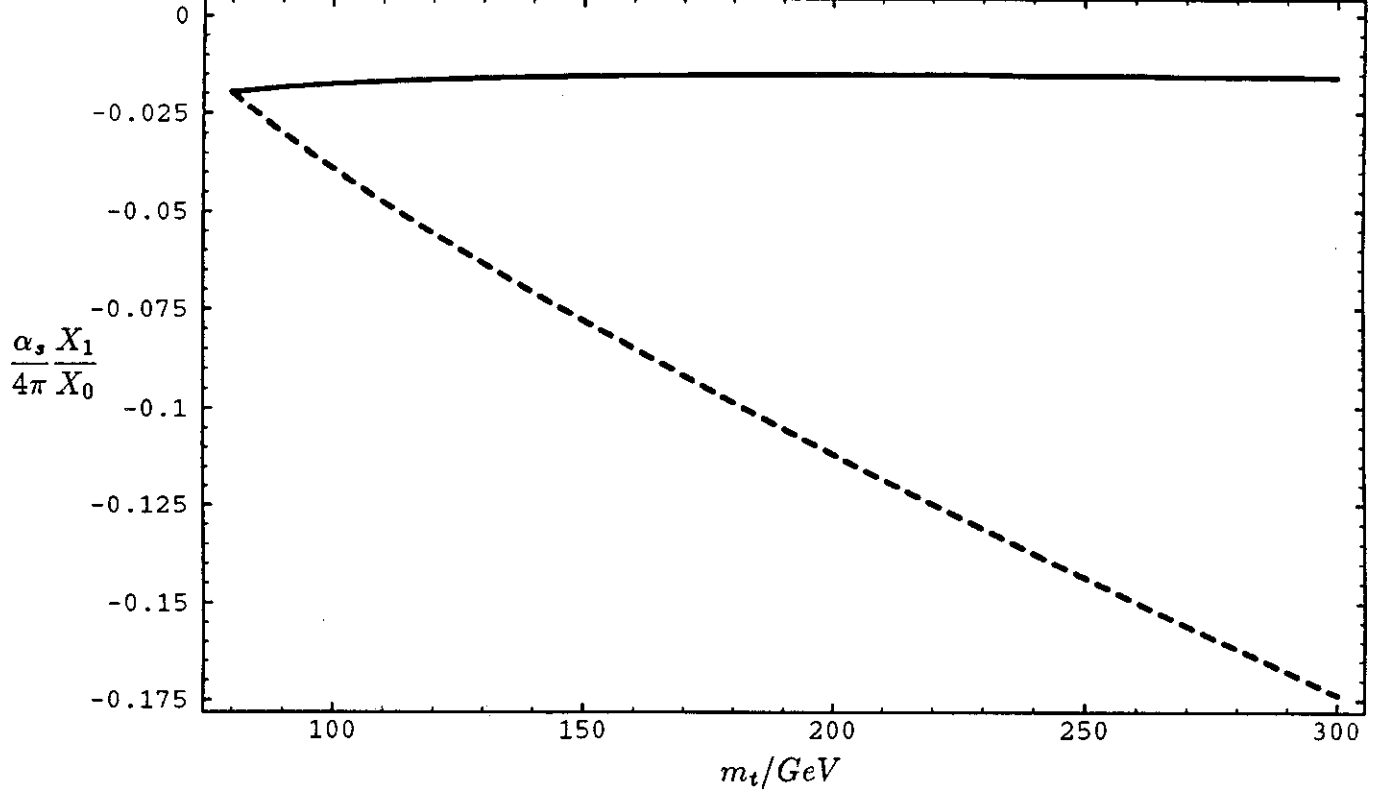


Fig. 3

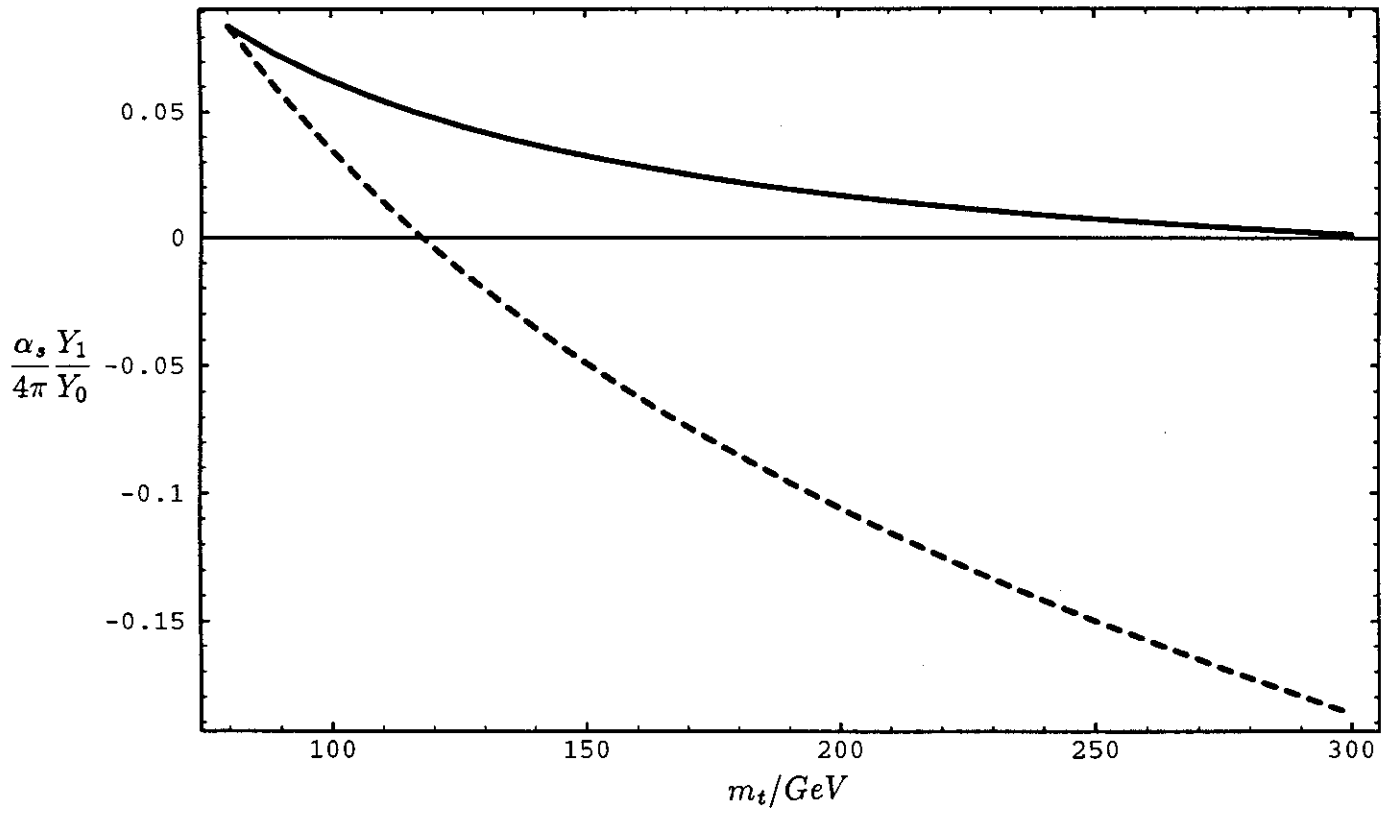


Fig. 4

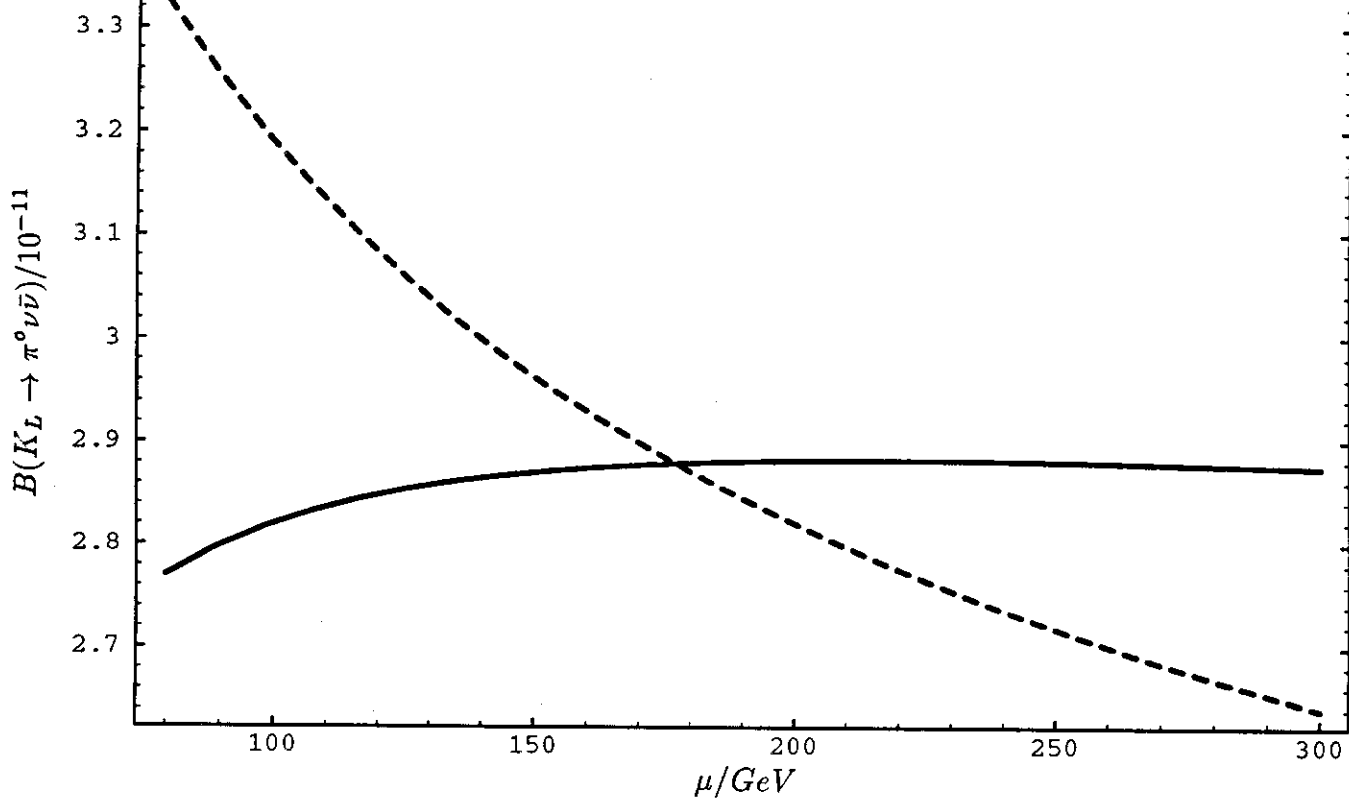


Fig. 5

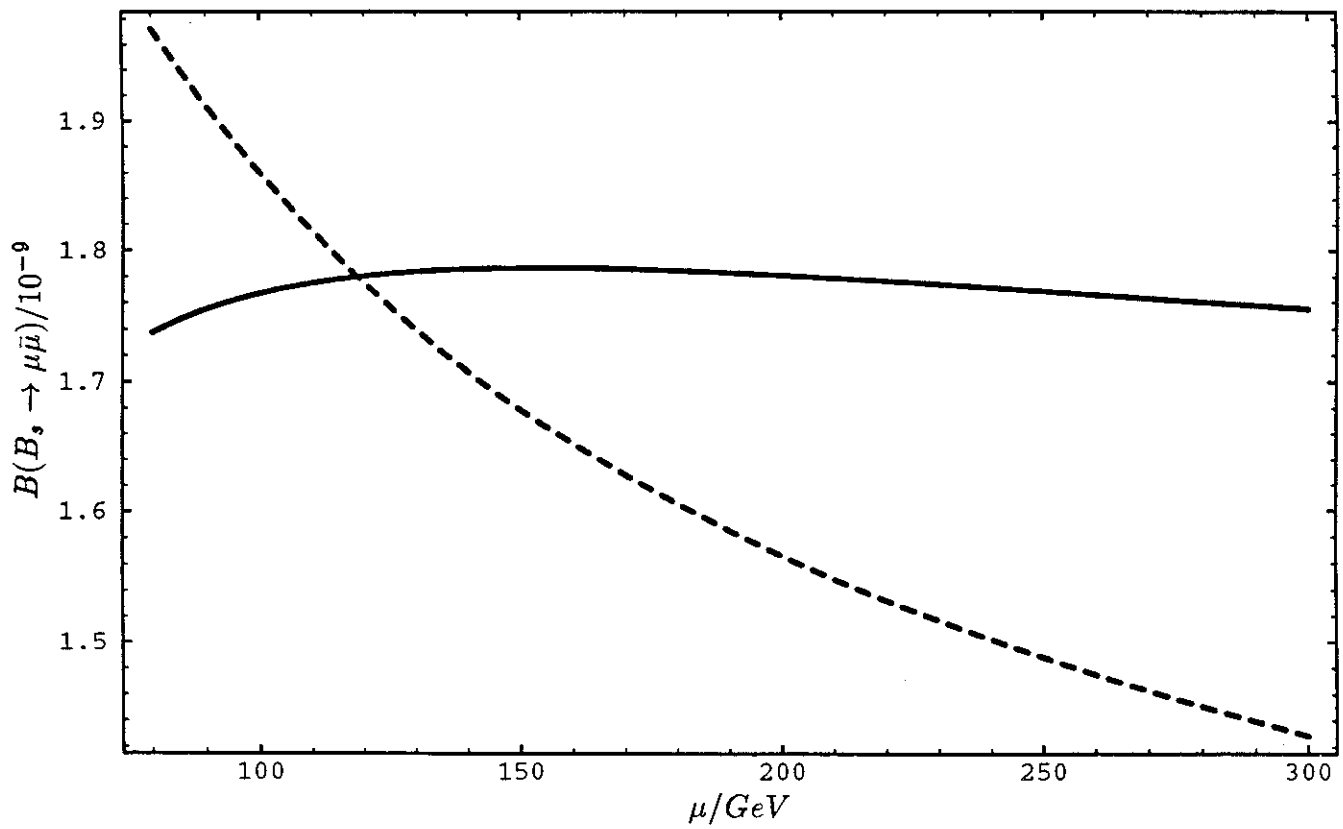


Fig. 6